LEAST SQUARES ESTIMATION METHOD FOR BASEMENT WAVES USING MULTI-DEPTH SEISMIC RECORDS

Masayuki YOSHIMI[1] and Hiromichi HIGASHIHARA[2]

[1] *Active Fault Research Center, Geological Survey of Japan, AIST, Tsukuba, Japan*
[2] *Earthquake Disaster Mitigation Research Center, NIED, Kobe, Japan*
Email: yoshimi.m@aist.go.jp, masayuki.yoshimi@gmail.com

ABSTRACT:
We propose a method for estimating basement waves based on least squares. In this method basement waves are determined from combination of borehole records at several depths and transfer functions. We validate this method by recovering observed ground motion of two well-investigated vertical arrays. It is confirmed that this new method stably recovers ground motions even for velocity structures with infinite quality factors.

KEYWORDS: ground motion, vertical array, velocity structure, Q value, soil response

1. INTRODUCTION

Estimation of engineering basement waves is one of the important tasks of seismic design. Regulation of nuclear power plant, for example, requires basement wave evaluation at a construction site. The basement motion is derived from borehole seismograms by removing local site effects. Thus validity of basement motion depends on accuracy of the subtraction of the local site effects.
Basement waves are usually estimated with a following procedure using vertical array records. Firstly velocity structure underneath a target site is investigated by prospection and seismograms analysis. Consequently, weak ground motion recorded at a reference depth is transferred to a basement wave applying investigated velocity structure with wave propagation analysis. Through this procedure estimation of basement wave may be distorted by the modeling error of the velocity structure and scatters involved in the selected ground motion. Especially when the attenuation is small, estimation is likely to instable.
In this article, we propose a feasible method to determine optimal target waves using borehole records at several depths.

2. ESTIMATION METHOD

Set [w] as a target wave. It can be any wave at a target site such as an incident wave at a certain depth or an engineering basement wave. Scattered or amplified with heterogeneous medium during propagation, [w] is converted into array observable waves [**u**]. So, [**u**]={**F**}[w], where {**F**} denotes an operator for transformation during wave propagation. If the operator {**F**} is known, [w] is determined from observed waves [**u**].
Now, consider a situation where the ground motion is weak enough to neglect nonlinear soil response. Assuming one-dimensional (1D) soil model along depth, {**F**}[w] is expressed as convolution, **F***w. Let T(f) be a Fourier transformed function of **F**, also, u_j and w, respectively, be a Fourier transformed observed wave at j-th seismograph and a Fourier transformed target wave, [w]. Then, optimal estimator of w is determined by solving the least squares problem

$$J = \sum_j \left\| u_j - T_j \hat{w} \right\|^2 \rightarrow min. \tag{2.1}$$

, where $\|*\|^2 \equiv \int_{-\infty}^{\infty} |*|^2$ and T_j is the frequency transfer function between input at the reference layer and output at the depth of the j-th seismograph.

Since the system is frequency independent, above problem is equivalent to

$$\forall f, J(f) = \sum_j \left| u_j(f) - T_j(f) w_j(f) \right|^2 \rightarrow min. \tag{2.2}$$

This yields the least squares estimators of the incident wave for each frequency,

$$\hat{w} = \frac{\sum_j T_j^* u_j}{\sum_j \left| T_j \right|^2} \tag{2.3}$$

, where T* denotes the conjugate of T.

Eqn. 2.3 shows that the optimal estimate of the target wave, w, is determined from combinations of observed waves at multiple depths and transfer functions.

In the following sections, we apply this estimation method to a site where the velocity structure is fully investigated and more than three borehole seismograms are installed at different layers.

3. ANALYSIS

3.1 data

We use ground motion records obtained at two borehole array sites, the Japan Atomic Energy Research Institute (JAERI) Oarai site (Ebisawa et al., 2001), and Nakao site in the dense array observation sites of Building Research Institute (BRI) in Sendai, Japan (Kitagawa et al., 1994). Figure 1 illustrates locations of Oarai (OAR: 36.262N, 140.549E) and Nakao in Sendai (NAKA: 38.254N, 141.007E), and epicenters of earthquake events used in this study. In both array sites, more than three seismographs have been installed in the boreholes to compose vertical array observation systems. Soil properties such as S-wave velocity and soil density have been obtained with S-wave loggings, soil tests, and soil behavior investigations. Table 1 lists one-dimensional (1D) velocity structure models based on S-wave loggings for OAR and NAKA together with depths of the seismographs.

3.2 settings

Estimation targets are records obtained at the deepest seismographs, GL -173 m for OAR and GL -61.0 m for NAKA. Horizontal records are converted into transversal component waves. Transfer functions are computed using 1D velocity model based on the 1D wave propagation theory. Least squares estimators are calculated based on the Eqn. 2.3 using one, two and three reference motions. Two sets of Q values, infinite Q and calibrated (or small) Q ($h=1/(2Q)=0.2f^{(-0.68)}$ for OAR, $h=1/(2Q)=0.091f^{(-0.459)}$ (Satoh et al., 1995) for NAKA), are assumed in order to test robustness of the estimations. Earthquakes are listed on Table 2.

4. RESULTS

4.1 OAR

Figure 2 left shows array records of EQ000051 at OAR. Middle and right in Figure 2 show estimated waves of the deepest seismogram (GL-173m) assuming infinite Q values and small Q values, respectively. Velocity response spectra of estimated motions and observed motion are shown in Figures 3 and 4 for infinite Q case and small Q case, respectively. Fittings of theoretical spectral ratios and observations for EQ000051 are shown in Figure 5.
It is noticed that even assuming infinite Q value, proposed method makes good estimation when three seismograms are used as reference (Ref3). In the small Q value case, all the estimations shows similar fit with slight overestimation.

4.2 NAKA

Figuer 6 left shows array records of A0400089 at NAKA. Middle and right in Figure 6 show estimated waves of the deepest seismogram (GL-61.0m) assuming infinite Q values and calibrated Q values (Satoh et al. 1995), respectively. Velocity response spectra of estimated motions and observed motion are shown in Figures 7 and 8 for infinite Q case and calibrated Q case, respectively. Fittings of theoretical spectral ratios and observations for A0400089 are shown in figure 9.
In the calibrated Q value case, both estimations (Ref1 and Ref2) show good agreement with the observation. On the other hand, in the infinite Q case, only the waves calculated using dual reference waves (Ref2) show good agreement with the target waves.

These results demonstrate that proposed method shows strong robustness against Q value.

5. SUMMARY

We developed a basement wave estimation method based on the least squares. Optimal estimator of a target wave is determined from combinations of observed waves at multiple depths and transfer functions. We applied the method to vertical array records at two well-investigated borehole sites, Oarai (OAR) and Nakao in Sendai (NAKA). We found that the new method provided reasonable estimation even with the velocity structure with infinite Q value, which may give rise to instable estimation with a conventional estimation method.

REFERENCES

Ebisawa, K., Yamada, H., Tsutsumi, H., Shibata, K., Ando, K., Baba, O. and Suzuki, H. (2001) Earthquake observation database in JAERI Oarai site obtained by vertical instrument arrays, JAERI-DATA/CODE, 2001-009, Japan Atomic Energy Research Institute, 97p.

Kitagawa, Y., Okawa, I. and Kashima, T. (1994) Dense array observation and analysis of strong ground motions at sites with different geological conditions in Sendai, *BRI Research Paper*, **139,** Ministry of Construction.

Satoh, T., Kawase, H. and Sato, T. (1995) Evaluation of local site effects and their removal from borehole records observed in the Sendai region, Japan, *Bull. Seism. Soc. Am.*, **85**, 1770-1789.

Satoh, T. (2006) Inversion of Qs of deep sediments from surface-to-borehole spectral ratios considering obliquely incident SH and SV waves, *Bull. Seism. Soc. Am.*, **96**, 943-956, doi: 10.1785/0120040179.

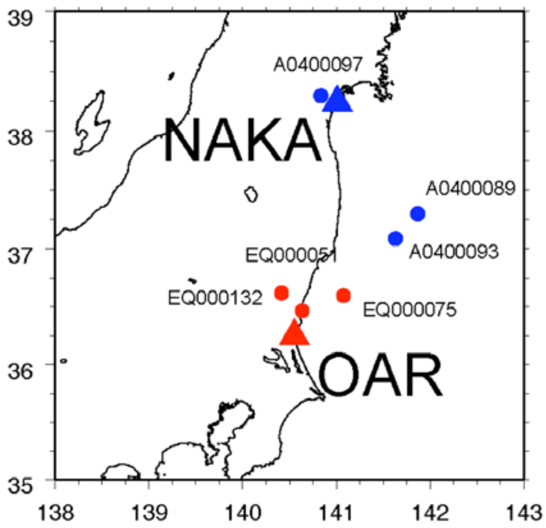

Figure 1 Site locations and epicenters

Table 1 1D velocity structure models

(a) OAR

Depth (m)	Thickness (m)	Density (kg/m3)	S-wave velocity (m/s)	Seismograph position
0.0	3.5	1.33	230	* GL -1.2
3.5	4.5	1.93	350	
8.0	1.5	1.78	300	
9.5	11.0	1.82	440	
20.5	6.0	2.05	650	
26.5	12.0	1.93	430	*GL -32.1
38.5	1.5	1.89	380	
40.0	24.5	1.85	370	
64.5	15.0	1.87	390	
79.5	11.0	2.02	490	
90.5	44.0	1.79	480	* GL -95.1
134.5	25.0	1.82	540	
159.5	15.5	1.86	590	* GL-173.0
175.0	-	1.99	1020	

(b) NAKA

Depth (m)	Thickness (m)	Density (kg/m3)	S-wave velocity (m/s)	Seismograph position
0.0	2.2	1.7	94	* GL -1.0
2.2	1.6	1.6	170	
3.8	1.8	1.8	170	
5.6	3.1	1.9	215	
8.7	6.8	1.9	215	
15.5	3.2	1.9	170	
18.7	5.1	1.7	170	
23.8	2.2	1.9	225	
26.0	3.0	1.7	225	
29.0	8.8	1.9	340	* GL -30.0
37.8	8.7	1.8	320	
46.5	11.3	2.0	490	
57.8	3.2	1.9	490	
61.0	-	2.0	720	* GL -61.0

Table 2 List of earthquakes

Name	Date Time (JST)	Location	depth	M_{JMA}	site	Distance (km)
EQ000051	1988/06/30 05:45	36.62N, 140.413E	52 km	4.2	OAR	41.4
EQ000075	1989/12/09 02:23	36.595N, 141.075E	46 km	5.6	OAR	59.9
EQ000132	1999/04/25 21:27	36.467N, 140.633E	58 km	5.1	OAR	23.9
A0400089	1987/04/07 09:41	37.3N, 141.867E	44 km	6.6	NAKA	130.2
A0400093	1987/04/23 05:13	37.088N, 141.627E	47 km	6.5	NAKA	140.5
A0400097	1989/06/24 04:59	38.297N, 140.83E	14 km	4.1	NAKA	16.2

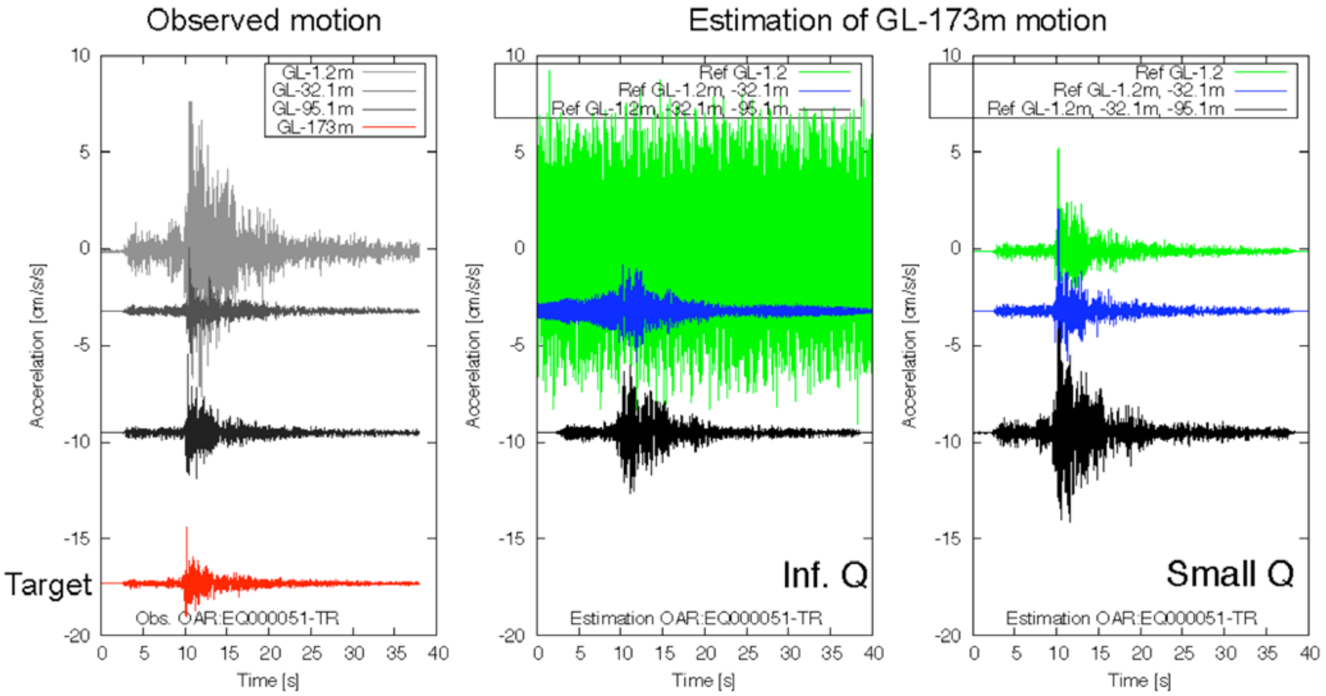

Figure 2 Array records (left) and estimated motions (middle: infinity Q case, right: small Q case) for EQ000051 at OAR.

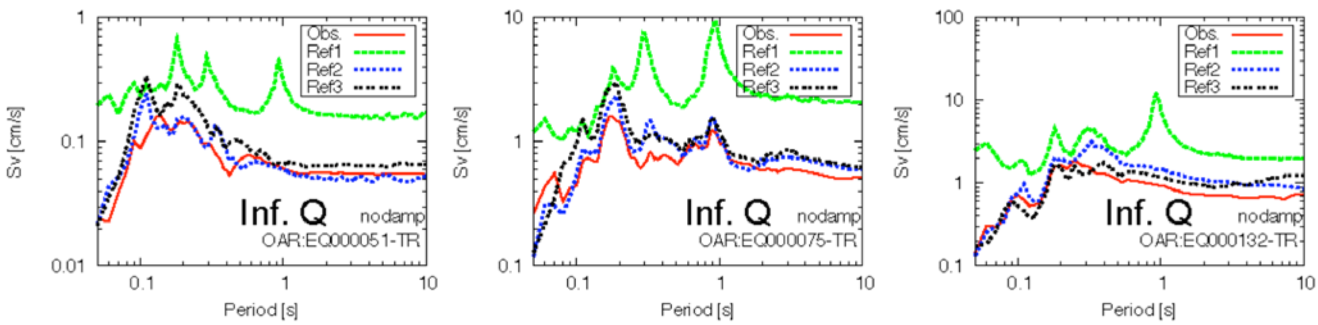

Figure 3. Comparison of velocity response spectra (h=0.05) of observed ground motion (Obs.) and estimated ground motions from one (Ref1), two (Ref2), and three (ref3) reference motions for site OAR, infinite Q. (left: EQ000051, middle: EQ000075, right: EQ000132)

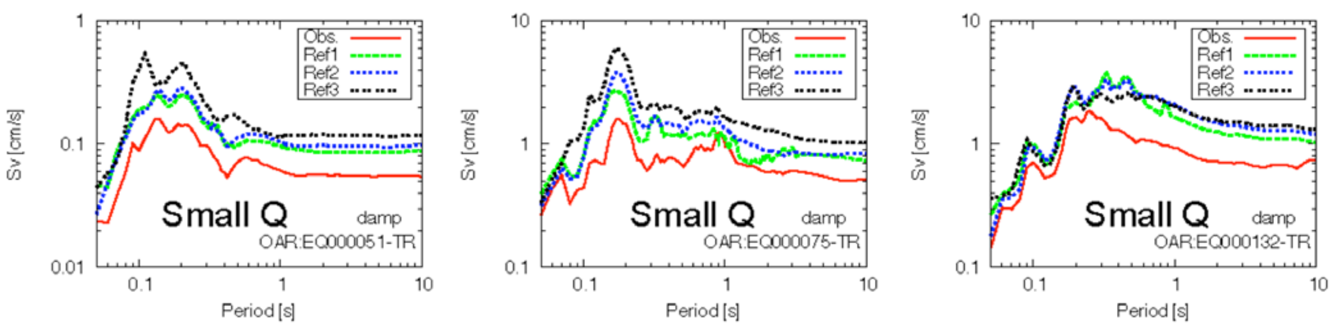

Figure 4. Same as Fig. 3, but for small Q values case.

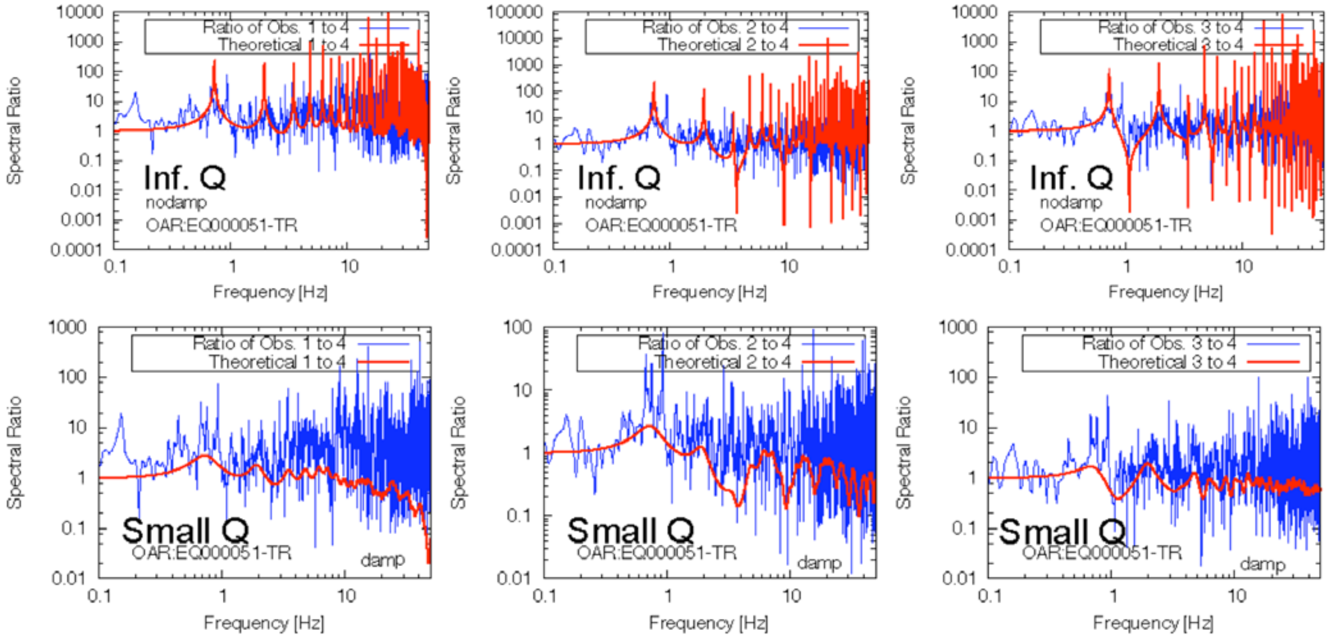

Figure 5. Comparisons of theoretical (red) and observed spectral ratios (blue) (Top: infinite Q, Bottom: small Q).

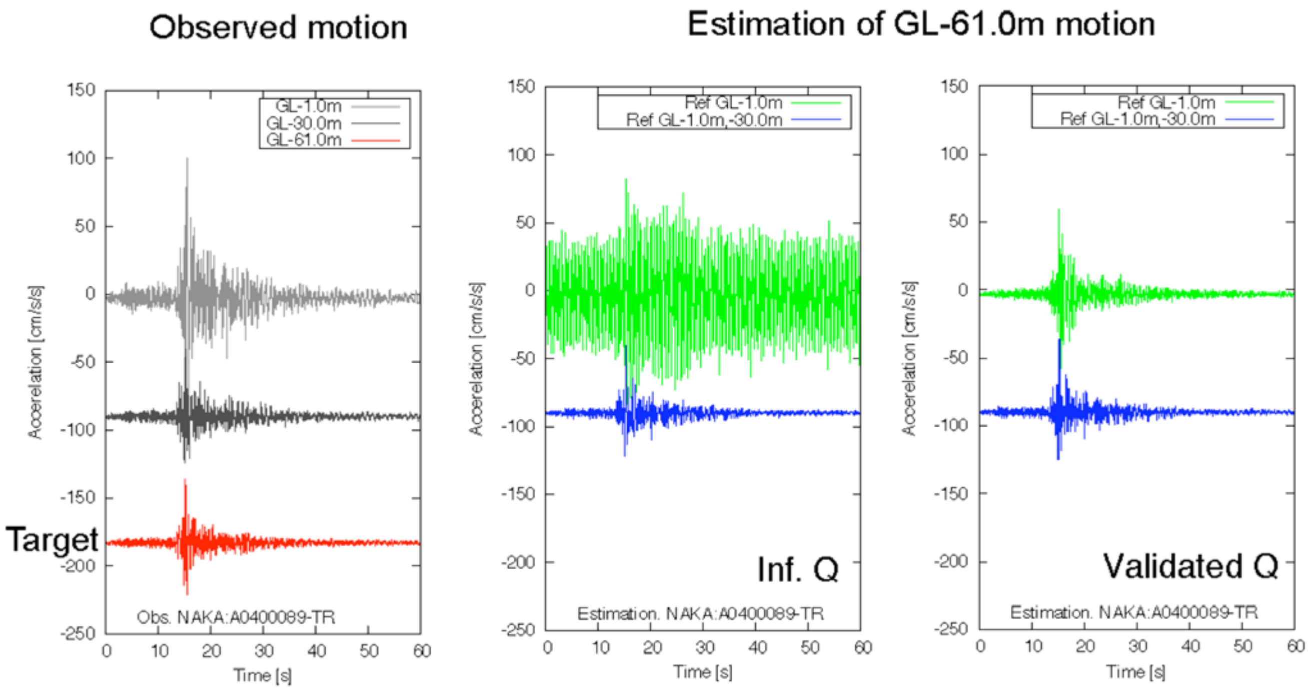

Figure 6 Array records (left) and estimated motions (middle: infinity Q case, right: small Q case) for A0400089 at NAKA.

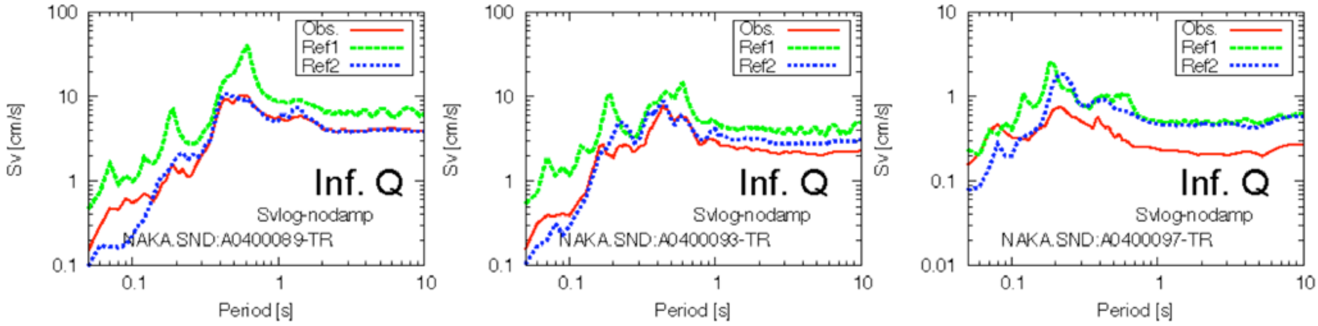

Figure 7. Comparison of velocity response spectra (h=0.05) of observed ground motion (Obs.) and estimated ground motions from one (Ref1), two (Ref2), and three (ref3) reference motions for site NAKA, infinite Q. (left: A0400089, middle: A0400093, right: A0400097)

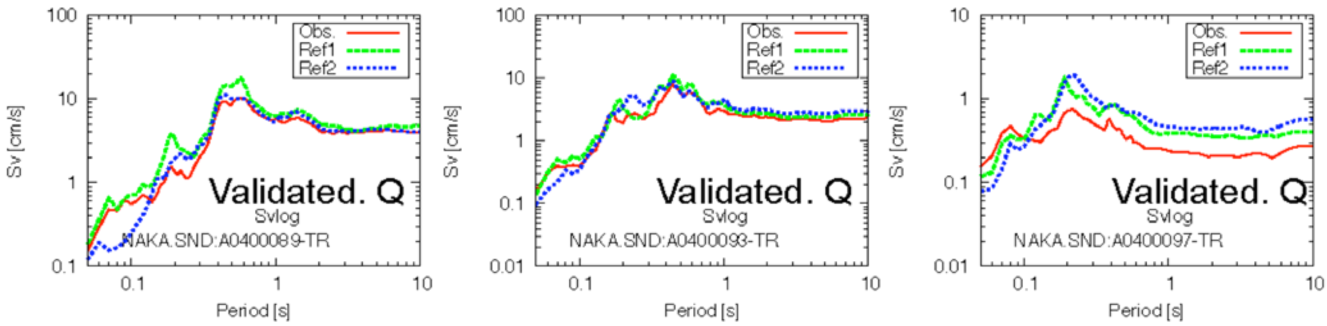

Figure 8. Same as Fig. 7, but for calibrated Q values case.

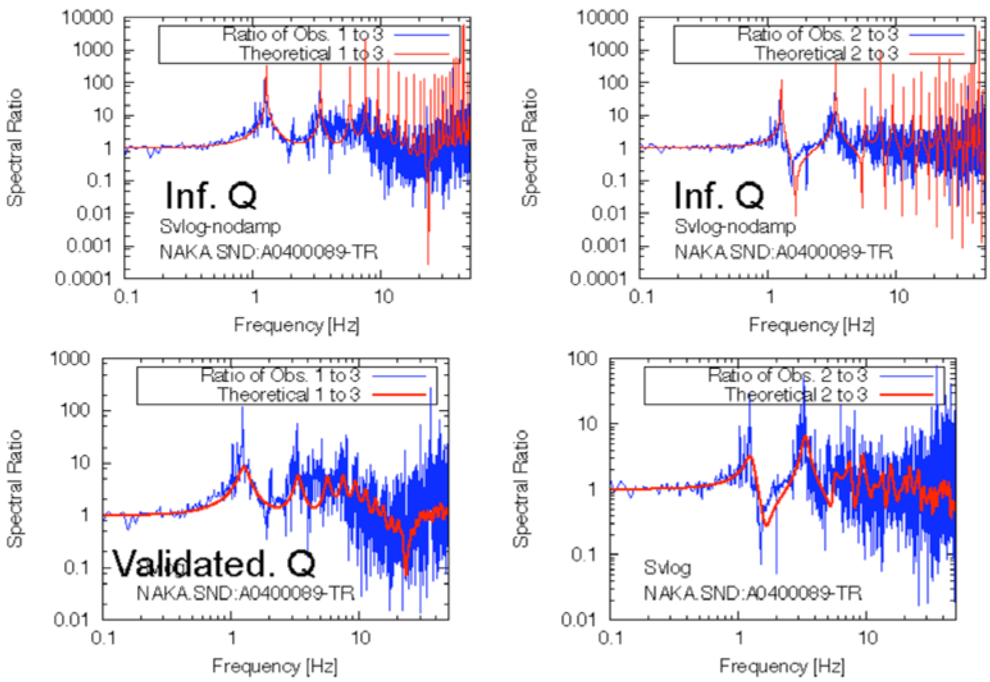

Figure 9 Comparisons of theoretical (red) and observed spectral ratios (blue) (Top: infinite Q, Bottom: calibrated Q).